Histol Histopathol (2017) 32: 627-637

http://www.hh.um.es

Histology and Histopathology

From Cell Biology to Tissue Engineering

Ghrelin and adipose-derived mesenchymal stromal cells improve nerve regeneration in a rat model of epsilon-caprolactone conduit reconstruction

Pedro Hernández-Cortés[1], Miguel Angel Toledo-Romero[2], Mario Delgado[3], Elena Gonzalez-Rey[3], Rafael Gómez Sánchez[1], Nicolás Prados-Olleta[4], José Aneiros-Fernández[5], Vicente Crespo-Lora[5], Mariano Aguilar[5], Pablo Galindo-Moreno[6] and Francisco O'Valle[5]

[1]Hand Surgery Unit, Orthopedic Surgery Department of San Cecilio University Hospital of Granada and Department of Surgery, University of Granada, Granada, [2]Hand Surgery Unit, Orthopedic Surgery Department of Virgen del Rocio University Hospital of Seville, Seville, [3]Institute of Parasitology and Biomedicine López-Neyra, CSIC, Granada, [4]Orthopedic Surgery Department of Virgen de las Nieves University Hospital of Granada, and Department of Surgery, University of Granada, Granada, [5]Department of Pathology, School of Medicine, and Biopathology and Regenerative Medicine Institute (IBIMER, CIBM), Granada and [6]Oral Surgery and Implant Dentistry Department, School of Dentistry, University of Granada, Granada, Spain

Summary. Objective. Attempts have been made to improve nerve conduits in peripheral nerve reconstruction. We investigated the potential therapeutic effect of adipose-derived mesenchymal cells (ASCs) and ghrelin (GHR), a neuropeptide with neuroprotective, trophic, and developmental regulatory actions, on peripheral nerve regeneration in a model of severe nerve injury repaired with nerve conduits.

Material and methods. The right sciatic nerves of 24 male Wistar rats were 10-mm transected unilaterally and repaired with Dl-lactic-ε-caprolactone conduits. Rats were then treated locally with saline, ASCs, or GHR. At 12 weeks post-surgery, we assessed limb function by measuring ankle stance angle and percentage muscle mass reduction and evaluated the histopathology, immunohistochemistry, ultrastructure, and morphometry of myelinated fibers.

Main Results. Rats receiving GHR or ASCs showed no significant increased functional recovery in ankle stance angle ($p=0.372$) but a higher nerve area ($p=0.015$), myelin area ($p=0.046$) and number of myelinated fibers ($p=0.012$) in the middle and distal segments of operated sciatic nerves in comparison to saline-treated control animals.

Conclusion. These results suggest that utilization of ghrelin or ASCs may improve nerve regeneration using Dl-lactic-ε-caprolactone conduits.

Key words: Epsilon-caprolactone, Ghrelin, Peripheral nerve injury, Nerve regeneration, Rat, Sciatic nerve

Offprint requests to: Prof. Francisco O'Valle, Departamento de Anatomía Patológica, Facultad de Medicina, Avda. de Madrid s/n, 18012 Granada, Spain. e-mail: fovalle@ugr.es

DOI: 10.14670/HH-11-828

Introduction

Improved understanding of the biological processes involved in nerve regeneration and the realization that nerve grafts serve as a guide for the growing neurons have led to the concept of entubulation techniques (Strauch, 2000; Babu et al., 2008). Although autologous nerve grafting remains the gold standard for nerve gap repair, artificial nerve conduits are considered a promising approach to peripheral nerve reconstruction (Strauch, 2000). However, conventional conduits fail to bridge large nerve defects (Meek et al., 2003), and various attempts have been made to overcome this shortcoming.

Advances in bioengineering have led to the creation of autodegradable composite neural tubes lined with Schwann cells or infused intraluminally with neurotrophic factors (e.g., NGF, VEGF, FGF), which enhance the regeneration of nerve fibers and block the invasion of scar tissue, improving outcomes (Ansselin et al., 1998; Hobson et al., 2000; Lee et al., 2003; Meek et al., 2003; Timmer et al., 2003; Belkas et al., 2005; Kim et al., 2007; Yu et al., 2009; De Boer et al., 2011).

Ghrelin (GHR) is a 28-aa neuropeptide that elicits a broad spectrum of biologic functions (Delporte, 2013). Initially related to appetite stimulation and growth hormone secretion, GHR has also been found to exert a neuroprotective effect in neurodegenerative diseases, regulate cognitive function, enhance synaptic function, and act as a potent neurotrophic factor in traumatic brain injury (Stoyanova et al., 2013; Qi et al., 2014). The positive effect of GHR on neural repair in the central nervous system is well documented, but its role in post-lesion peripheral nerve regeneration is poorly understood. Preliminary data suggest that GHR may play a role in promoting axonal regeneration after nerve injury (Raimondo et al., 2013). Moreover, administration of GHR prevented diabetes-induced polyneuropathy (Tsuchimochi et al., 2013) and reduced axonal damage and neuropathic pain in a model of chronic constriction injury of the sciatic nerve (Guneli et al., 2010), apparently through its effect on inflammatory and oxidative responses.

ASCs have various characteristics that make their use attractive in the setting of peripheral nerve damage. First, they can differentiate to Schwann cells and produce trophic factors involved in nerve regeneration; second, they show preferential homing for sites of inflammation and tissue damage, as in an injured nerve (Gonzalez et al., 2009); third, they exert potent immunosuppressive and antifibrotic actions, favoring nerve repair; and fourth, ASCs can be used in an allogeneic system, extending the applicability of this strategy. Infusion of ASCs or other mesenchymal stromal cells (MSCs) to nerve conduits has improved nerve repair in various experimental models (di Summa et al., 2010; Ao et al., 2011; Carriel et al., 2013).

We investigated two different therapeutic approaches to the improvement of peripheral nerve reconstruction: a molecular strategy that uses endogenous factors such as the anti-inflammatory and neuroprotective neuropeptide GHR; and a cellular strategy that uses ASCs. The objective of the present study was to compare the regeneration of injured peripheral nerves between nerve conduits treated with GHR or ASCs and conduits treated with saline (controls).

Materials and methods

Experimental animals

We used 24 Wistar male rats weighing 300-350 g, kept under stable conditions with ad libitum access to food and water. All experiments were performed in a homologated laboratory according to the European Union and Spanish Government guidelines for the ethical care of animals (EU Directive 63/2010, RD 53/2013), and the study was approved by the ethical commission for animal research of our institution.

We studied a unilateral peripheral nerve injury model, using Dl-lactic-ε-caprolactone conduits (CC) (Neurolac®, Polyganics, Groningen, Holland) to repair a 10-mm defect in sciatic nerve of rat (Fig. 1). Animals were randomly assigned to three groups that were exposed to different treatments of the defect: CC group (n=8), in which treatment consisted of simple entubulation with a 2-mm wide and 15-mm long Dl-lactic-ε-caprolactone conduit plus saline; CC-GHR group (n=8), repaired as in the CC group plus instillation of 3 μg of ghrelin (AnaSpec, San Jose, CA, USA) (dissolved in 100 μL of saline at 30 μg/mL) weekly from weeks 2 to 6 at a subcutaneous site above the muscle over the region containing the conduit, using a temporary subcutaneous catheter that was in place during the 6-week period. CC-ASC group (n=8), repaired as in the CC group plus intratubular inoculation of 10^5 ASCs per conduit.

Experimental procedure

Animals were anesthetized with diethyl ether (Sigma-Aldrich, Barcelona, Spain) inhalation followed by intraperitoneal injection of a solution of ketamine (1 mL), diazepam (0.8 mL), and atropine (0.2 mL) at a dose of 3 mL/kg. Preoperative anti-infectious prophylaxis was conducted by administering 30 mg/kg of intramuscular cefuroxime. For postoperative analgesia, the rats received metamizole (200 mg/kg, po) directly after waking and buprenorphine (50 mg/kg, sc) every 12 hrs for 3 days.

The right sciatic nerve was exposed between the *vastus lateralis* and *biceps femoris* by longitudinal posterolateral incision. The nerve was then dissected from the surrounding tissue with a surgical microscope, and a 1-cm portion was resected using microsurgical instruments (Fig. 1). The nerve defect was reconstructed with a 2-mm wide and 15-mm long Dl-lactic-ε-caprolactone conduit in the CC, CC-ASC, and CC-GHR groups.

Preparation of mesenchymal stem cells from adipose tissue (ASCs)

Abdominal (epididymal) and subcutaneous (inguinal) fat was aseptically removed from male Balb/c mice (10-12 weeks old, Charles River, France), as previously described (Gonzalez-Rey et al., 2009), and washed twice in Hank's balanced salt solution (HBSS; Invitrogen, Dun Laoghaire, Dublin, Ireland). The fat tissue was weighed, cut into small pieces (2 mm^3), and resuspended in 2.5 mL of HBSS containing 2 mg/mL collagenase type I (Sigma-Aldrich, Barcelona, Spain) per gram fat tissue and incubated for 30 minutes at 37°C, swirling the tube every 5 minutes. The digest was washed twice with 10 mL HBSS and filtered each time through a 100-µm nylon mesh. Finally, cells were resuspended in complete MesenCult (Stem Cell, Grenoble, France) medium containing 100 units/mL penicillin/streptomycin (Gibco, Invitrogen, Madrid, Spain) and 20% mouse mesenchymal supplements (Stem Cell) and were plated at a density of 15,000-30,000

cells/cm^2 and cultured in a 20%O_2/5%CO_2 atmosphere. Non-adherent cells were removed after 24 hours in culture. Subsequent passages were plated at 10,000 cells/cm^2 in complete MesenCult medium. ASCs were used between passage 3-7. These cells showed a fibroblast-like morphology and capacity to differentiate into adipocytic and osteocytic lineages (Gonzalez-Rey et al., 2009; Araña et al., 2013).

Functional assessment

Among the numerous available gait parameters, ankle stance angle (ASA) was selected to evaluate functional recovery. ASA is the ankle joint angle measured at the mid-stance phase of the step cycle and is formed by two lines, one that is parallel with the tibial axis and the other that connects the lateral malleolus to the head of the fourth metatarsal. Gait movements were recorded with a video camera (Sony DCR-DVD92E) mounted at a distance of 100 cm at right angles to the running direction of the rat. The procedure was stopped when five complete gait cycles were recorded on the tape. The analysis did not include the step cycles when the rat first began to walk or immediately before the rat stopped walking. The recordings were then digitalized, and three images per animal were captured with Windows Movie Maker software (version 2011 [compilation 15.4.3502.0922] Microsoft Corporation, Redmond, WA, USA). For each animal, the ASA was calculated pre- and post-surgery as the average of three individual measurements.

The animals were euthanized at 12 weeks post-surgery by CO_2 inhalation. The sciatic nerves on both sides and the surrounding soft tissues were then extracted *en bloc*. The nerve on the left side served as internal control. The soleus and gastrocnemic muscles of both hind limbs were collected and weighed. The percentage muscle mass reduction was calculated by subtracting the weight of muscle in the intervened limb from the weight of the muscle in the control limb, dividing by the weight of the muscle in the control limb and multiplying by 100 (see Table 1 footnote).

Histopathological, morphometric, and immunohistochemical study

For the histopathological study, cross-sections at the proximal segment, mid-tube segment, and distal part of the sciatic nerve-muscle complex of the rear limb were fixed in 10% buffered formalin, embedded in paraffin, and cut in 4-μm sections. Dewaxed and hydrated tissue sections were then stained with hematoxylin-eosin (H&E), PAS, Masson's trichrome, and Kluver-Barrera (K-B). For the immunohistochemical assessment, tissue sections were heat-treated in 1 mM EDTA buffer for antigenic unmasking (PT module device, Thermo Fisher Scientific, Kalamazoo, MI, USA) at 95°C for 20 min. Sections were then incubated for 10 min at room temperature with prediluted anti-myelin basic protein polyclonal antibody in an automatic immunostainer (Autostainer480S, Thermo Fisher Scientific) using the micropolymer-peroxidase-based method (Ultravision Quanto), followed by development with diamino-benzidine. All reagents were purchased from the same company (Master Diagnóstica, Granada, Spain). Data were gathered on the presence of myelinated fibers in distal nerve, neuroma changes, and a semiquantitative score of myelin basic protein immunostaining intensity (0: absent, 1: low, 2: medium, and 3: intense).

A millimeter scale in the eyepiece of a BH2 microscope with a 40x objective (Olympus Optical Company, Ltd., Tokyo, Japan) was used to count in 20 fields the number of myelinated fibers per mm^2 of myelinated fibers in the proximal, mid-tube, and distal segments of the operated nerves and in the proximal and distal segments of the non-operated (control) nerves as well as *triceps surae* muscle fibers.

Tissue sections were stained with 1% picro Sirius red F3BA (Gurr, BDH Chemicals Ltd., Poole, United Kingdom) for perineural fibrosis image analysis quantification. The staining was enhanced by immersing deparaffinized tissue sections for 3-5 days in 70% ethanol as mordant. Picro Sirius red stains connective fibers deep red and cell nuclei and cytoplasmic structures light red/bright yellow. Fibrosis was quantified by assessing 20 images per sample with a Sony camera connected to a BX-41 microscope (Olympus Optical Company) with an MTV-3 adapter, using a 3.3x intermediate lens and 20x objective. Images were processed and automatically quantified with the Fibrosis HR® program (ImaGesp, Barcelona, Spain) (Masseroli et al., 1998).

The same morphometric system was used to measure the following parameters: 1) the area of the nerves occupied by myelinated fibers in the proximal, mid-tube, and distal areas of the nerve in K-B-stained and myelin basic protein-stained sections; 2) the area of muscle occupied by fibers (H&E staining) in the central portion of cross-sections of the muscle mass. Muscle fiber reduction was assessed as mean percentage reduction with respect to the contralateral (control) *triceps surae* muscle (control fiber area-problem fiber area/control fiber area, multiplied by 100).

The muscle fiber area was measured using the same method, calculating the mean percentage reduction with respect to the contralateral (control) *triceps surae* muscle (control fiber area-problem fiber area x 100/control fiber area). In all cases, a medial cross-section was taken using a special clamp for 2-mm thick parallel sections (CutMATE, Milestone, Kalamazoo, MI, USA).

Electron microscopic study

Several 1-mm^2 fragments of sciatic nerve from multiple proximal, mid-tube, and distal segments were fixed in 2.5% glutaraldehyde solution and then postfixed in 1% OsO_4 at 4°C for 2 h, washed in distilled water, dehydrated in increasing concentrations of acetone, and

embedded in Epon following a conventional protocol. Semithin sections were stained with toluidine blue solution. Ten blocks of each area were sampled.

Ultrathin (~70 nm-thick) sections were obtained in a Reichert Jung ULTRACUT ultramicrotome (Leica, Wetzlar, Germany) and stained with lead citrate and uranyl acetate. Ultrathin sections were examined under a Zeiss EM 902 transmission electron microscope and processed using specific software for Windows (Soft Imaging System, Berlin, Germany). The number of myelinated axons, the myelin sheath area, and g-ratio (ratio of inner axonal diameter to total outer diameter) in randomly selected nerve sections were determined by examination at equal magnification (1995 nm) and were assessed using ImageJ v.1.4 software (http://imagej.nih.gov/ij/) (Bethesda, MD, USA).

Statistical analysis

IBM SPSS (v. 20.0; IBM SPSS, Armonk, NY, USA) was used for the statistical analysis. The Kruskal-Wallis test was applied to compare functional, histopathological, and morphometric data among the groups, and the Dunn-Bonferroni *post hoc* test was used to compare pairs of groups when a significant difference was detected; the Mann-Whitney U-test was used for non-parametric variables. Spearman correlation coefficients were calculated between functional and histomorphometric variables. The confidence interval was 95% ($p<0.05$).

Results

Surgical outcomes

All animals survived the surgery, and none evidenced infection or other apparent complications. Five of eight rats in CC group, three in CC-ASC group, and four in CC-GHR group had neurotrophic ulcers in the heel of the intervened limb and mild/moderate distal edema within two postoperative weeks. The most intense lesions, including mutilations, were observed in the CC group (3/8 rats). Ulcers in animals from the CC-GHR and CC-ASC groups healed spontaneously within 12 weeks.

Functional recovery

Postoperative examination of knee and ankle movements showed a complete loss of function of both flexor and extensor muscles in the shank. The mean ASA significantly decreased from 62.94°±2.96° (before surgery) to 36.85°±4.10° three weeks post-surgery in all experimental groups [Mann-Whitney U-test, $p<0.05$]. At 12 weeks post-surgery, functional recovery was scant, and there was no statistically significant difference in ASA among the three groups (Kruskal-Wallis $p=0.372$) (Table 1).

Assessment of muscle atrophy

All animals showed moderate/severe macroscopic muscle atrophy in the operated limb at 12 weeks in comparison to the non-operated limb, although no difference was found among the groups in wet weight reduction of the *triceps surae* (Kruskal Wallis test; $p=0.130$; Table 1). Notably, treatment of the entubulated nerves with GHR or ASCs significantly attenuated the reduction in muscle fibers induced by the injury (Kruskal Wallis test, $p=0.012$; Table 1).

Histologic, ultrastructural and morphometric assessment

All groups showed histologic evidence of nerve tissue at the proximal, mid-tube (Fig. 2), and distal areas. Except for one case of collapse (in the CC group), the lumen of nerve conduits was preserved and partially occupied by nerve fibers, with no fascicular organization

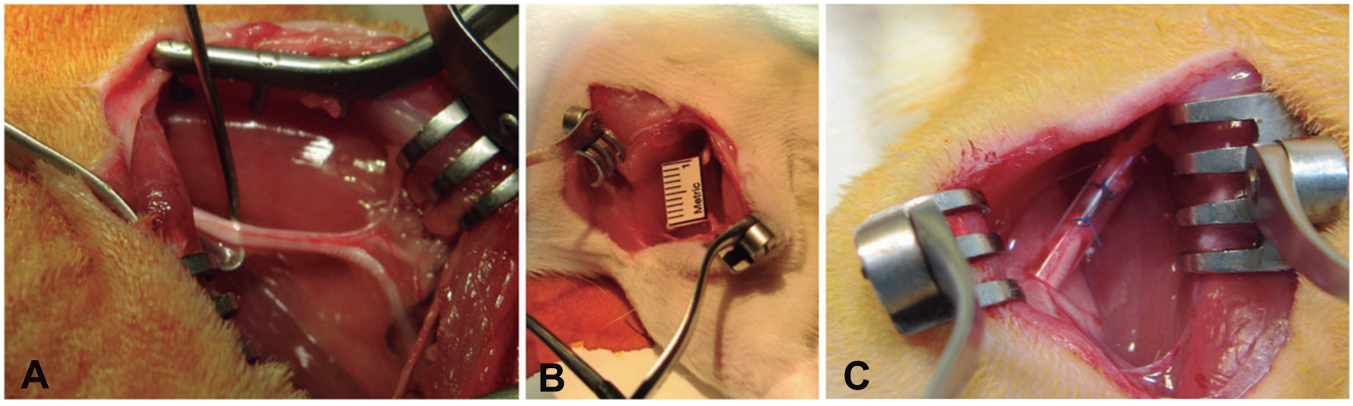

Fig. 1. Model of sciatic injury defect in Wistar rat. **A.** Sciatic nerve between the vastus lateralis and biceps femoris exposed by longitudinal posterolateral incision. **B.** Sciatic nerve showing a 10-mm defect. **C.** Reconstruction of the nerve by suture under tension with a 15-mm long Dl-lactic-ε-caprolactone conduit.

or connective tissue. The wall of the conduit was in most cases fragmented, partially destructured, and surrounded by connective and granulomatous tissue, with the presence of giant multinucleated cells (Fig. 2). No statistically significant differences were found among groups in the myelinated fiber count, myelinated area, or g-ratio in the proximal segment of the sciatic nerve (Kruskal Wallis, p=0.529, p=0.109, p=0.904, respectively). K-B histochemical analysis (Table 1, Fig. 2) showed significant differences among experimental

Table 1. Statistical comparision of the functional, morphological and immunohistochemical values.

	CC group	CC-GHR group	CC-ASC group	P-values (K-W)
ASA	40.84°±4.26°	49.70°±9.21°	45.71°±9.35°	p=0.372
Ms W reduction (%)	62.41±24.93	56.10±9.85	58.01±6.79	p=0.130
Myelinated fibers /mm^{2*}	6201±3814	8366±5492	7683±4321	p=0.032
Myelinated fibers /mm^{2**}	3006±2520	10352±2155	6500±1022	p=0.000
MBP fibers/mm^{2*}	3971±1957†	7541±3146	7013±5195	p=0.031
MBP fibers/mm^{2**}	3876±1874‡	7666±2963	7278±3848	p=0.019
Nerve area mm^{2*}	0.42±0.27	0.46±0.18	0.40±0.25	p=0.996
Nerve area mm^{2**}	0.44±0.35	1.07±0.45	0.87±0.40	p=0.015
Perineural fibrosis mm^{2*}	0.23±0.33	0.25±0.15	0.35±0.10	p=0.642
Perineural fibrosis mm^{2**}	0.45±0.80	0.25±0.17	0.25±0.13	p=0.018
Muscle fiber reduction (%)	65.31±52.57	16.30±12.44	24.5±15.18	p=0.012

CC Group: control group (nerve lesion repaired by simple entubulation). CC-GHR Group: nerve lesion repaired by entubulation with Ghrelin instillation. CC-ASC Group: nerve lesion repaired by entubulation with conduits seeded with adipose-derived mesenchymal stem cells (ASCs). * mid-tube, and ** distal segment values (CC Group n=7 rats). K-W: Statistical significance by Kruskal-Wallis test. ASA: ankle angle in midstance phase of the gait at 12 weeks post-surgery. Mean of three measurements per rat. Ms W Reduction: weight of the triceps surae of the control limb subtracted by weight of the triceps surae of the intervened limb, divided by weight of the triceps surae of the control limb and multiplied by 100. Myelinated fibers /mm^2: number of myelinated fibers per mm^2 in mid-tube and distal nerve segments. MBP fibers/mm^2: number of myelin basic protein positive fibers per mm^2 in mid-tube and distal nerve segments. †CC vs CC-GHR-group (p=0.028, Dunn-Bonferroni test); ‡CC vs CC-GHR-group (p=0.017, Dunn-Bonferroni test). Nerve area mm^2: area of the nerve in midtube nerve segment, calculated automatically by Fibrosis HR® software. Perineural fibrosis mm^2: area of connective tissue surrounding the nerve, calculated automatically by Fibrosis HR® software in mm^2. Muscle fiber reduction (%): Mean percentage reduction with respect to the contralateral (control) triceps surae muscle (control fiber area-problem fiber area/control fiber area, multiplied by 100). Mean values ± standard deviation of the series (n=8 rats per group).

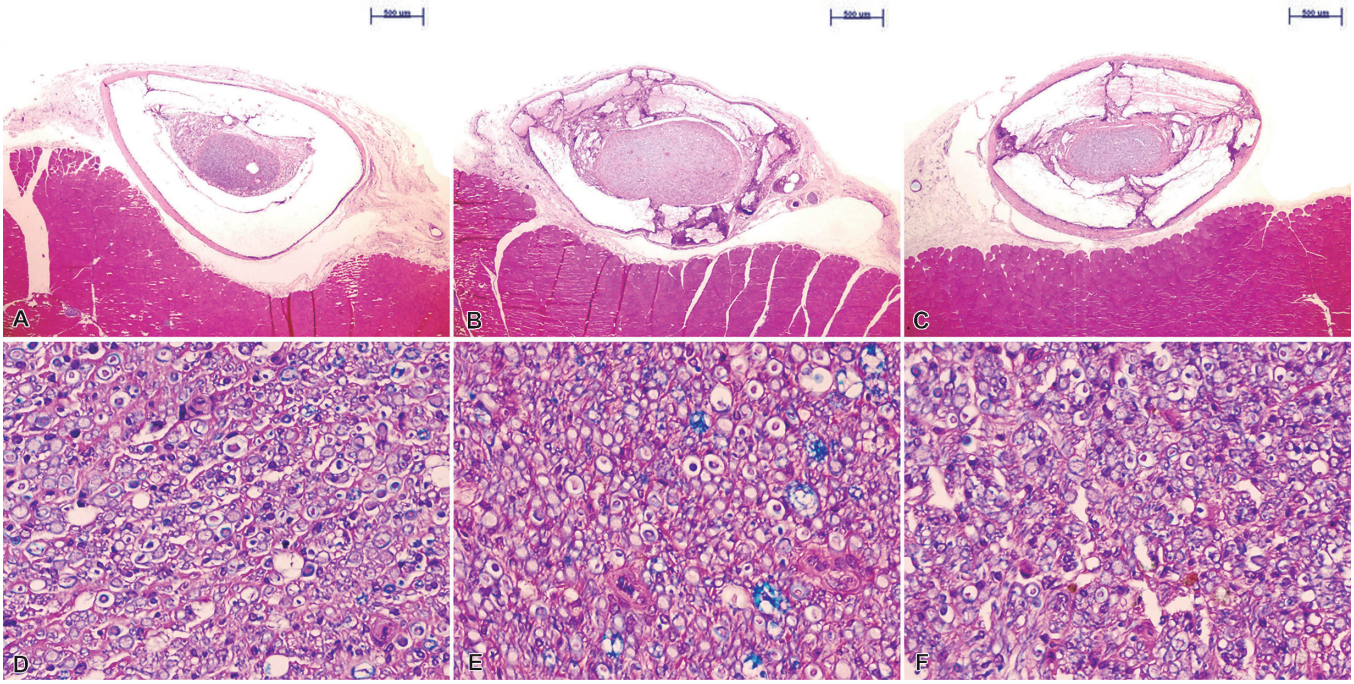

Fig. 2. Cross-sections of the middle portion of conduits of the sciatic nerve isolated from CC group (**A and D**), CC-GHR group (**B and E**), and CC-ASC group (**C and F**) stained with the Kluver-Barrera method. A-C, x 2; D-F, x 40

groups in the myelinated axon count per mm^2 in the middle segment of regenerated nerve fibers (Kruskal Wallis test, p=0.032). The distal portion of the nerve evidenced degenerative phenomena, partial substitution by connective tissue, and some regenerated nerve fibers. Treatment with GHR or ASCs significantly improved the remyelination process in middle and distal segments (Tables 1-3). These findings were confirmed by immunohistochemical analysis of myelin basic protein-positive nerve fibers in the distal segment (Fig. 3; Kruskal Wallis test, p=0.019) and by ultrastructural quantification of the myelinated area (Fig. 4; Kruskal Walli test p=0.002), myelinated fiber count (Table 2; Kruskal Wallis test, p=0.000), and remyelination (g-ratio) (Table 3; Kruskal Wallis test, p=0.047). Thus, the ASCs and GHR-treated animals had more myelinated fibers in middle (Kruskal Wallis test, p=0.012) and distal (Kruskal Wallis test, p<0.001) nerve segments in comparison to the untreated controls. Interestingly, the three experimental groups showed a similar mid-tube presence of perineural connective tissue (Table 1; Kruskal Wallis test, p=0.642), while its presence was

Table 2. Statistical comparision of the nerve ultrastructural morphometric study by digital image analysis.

	CC group	CC-GHR group	CC-ASC group	P-values (K-W)
No. myelinated fiber (mid-tube)	27.21±11.15	38.38±14.20	37.50±15.42	p=0.012
No. myelinated fiber (distal)	21.10±7.21	35.89±3.23	35.89±14.6	p=0.000
No. unmyelinated fiber (mid-tube)	21.07±19.18	11.99±4.80	12.80±5.23	p=0.042
No. unmyelinated fiber (distal)	17.51±6.35	13.35±7.14	13.69±5.11	p=0.653
Myelin (%) (mid-tube)	21.09±9.19	24.61±9.03	22.34±8.03	p=0.789
Myelin (%) (distal)	10.06±5.75	18.29±6.66	14.84±3.09	p=0.072
Myelin area (μm^2) (mid-tube)	0.12±0.14	0.27±0.13	0.24±0.15	p=0.046
Myelin area (μm^2) (distal)	0.09±0.04	0.25±0.08	0.22±0.21	p=0.002

CC Group: control group (nerve lesion repaired by simple entubulation). CC-GHR Group: nerve lesion repaired by entubulation with Ghrelin instillation. CC-ASC Group: nerve lesion repaired by entubulation with conduits seeded with adipose-derived mesenchymal stem cells (ASCs). K-W: Statistical significance by Kruskal-Wallis test. Number of myelinated and unmyelinated axons, percentage and area of myelin: number of myelinated axons, percentage and area of the nerve in mid-tube nerve and distal segments (CC Group n=7 rats), calculated semiautomatically by ImageJ® software in ultrastructural study. Mean values ± standard deviation of the series (n=8 rats per group).

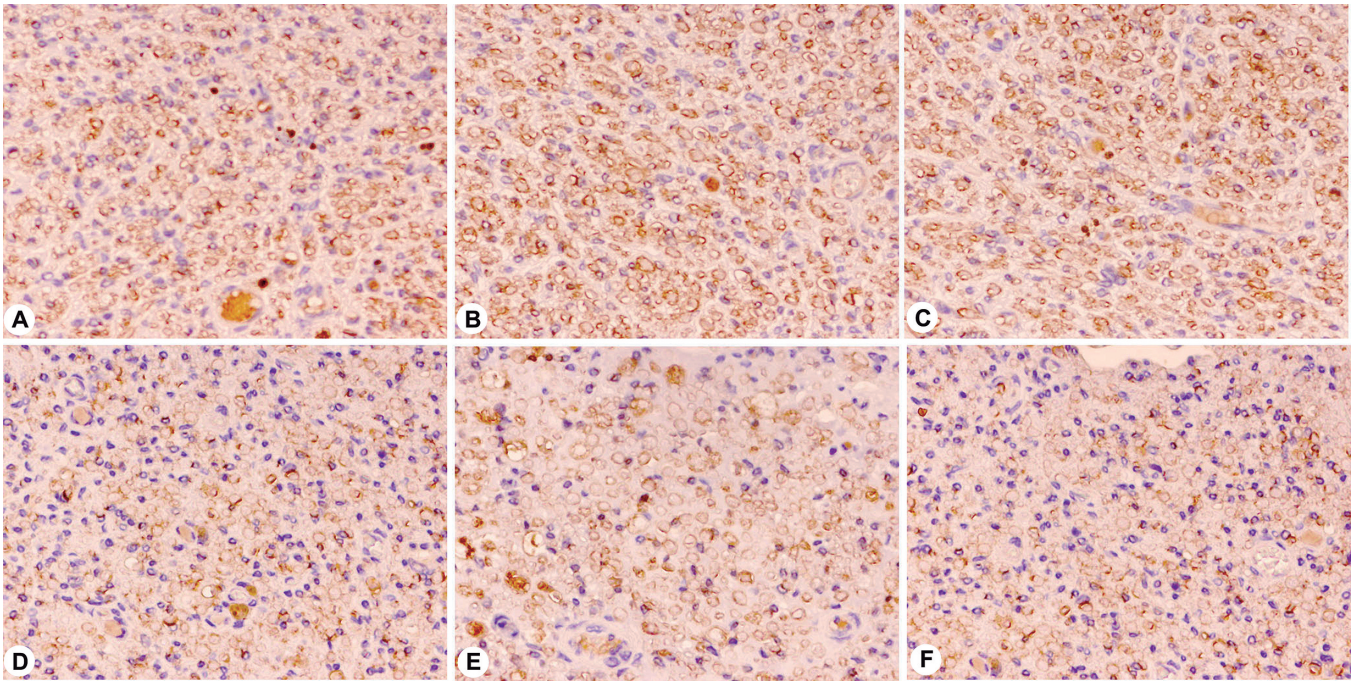

Fig. 3. Immunohistochemical analysis of myelin basic protein expression (brown staining) in cross-sections of the sciatic nerve in the middle portion of conduit **(A-C)** and distal segment **(D-F)** isolated from CC group **(A and D)**, CC-GHR group **(B and E)** and CC-ASC group **(C and F)**. Micropolymer-peroxidase-based method. x 40

lesser in the distal segment (Table 1; Kruskal Wallis test, p=0.018) in CC-GHR and CC-ASC-groups in comparison to the untreated controls (Dunn-Bonferroni test, both p=0.040).

We also observed significant negative correlations between the myelinated axon count per mm^2 and nerve area in the distal segment of the operated nerve and the wet weight reduction in soleus and gastrocnemic muscles (Spearman's rank correlation coefficient Rho: -0.673, p=0.001; Rho: -0.463, p=0.046, respectively). No significant correlation was observed between ASA and myelinated axon count per mm^2 in the distal segment of the operated nerve (Spearman's rank correlation coefficient Rho: 0.013, p=0.956), nerve area (Spearman's rank correlation coefficient Rho: -0.267, p=0.273), or perineural fibrosis area (Spearman's rank correlation coefficient Rho: -0.322, p=0.154); or in the percentage muscle wet weight reduction (Spearman's rank correlation coefficient Rho: 0.016, p=0.944). However, the ASA was correlated with the myelinated

Table 3. Statistical comparisionof g-ratio in the nerve ultrastructural morphometric study.

	CC group	CC-GHR group	CC-ASC group	P-values (K-W)
Total outer diameter (proximal) (µm)	0.94±0.33*	0.88±0.37	0.88±0.35	p=0.863
Inner axonal diameter (proximal) (µm)	0.63±0.21	0.61±0.29	0.60±0.23	p=0.957
g-ratio (proximal)	0.67	0.69	0.68	p=0.904
Total outer diameter (mid-tube) (µm)	0.56±0.13	0.54±0.34	0.66±0.13	p=0.153
Inner axonal diameter (mid-tube) (µm)	0.41±0.15	0.28±0.17	0.43±0.12	p=0.910
g-ratio (mid-tube)	0.73†	0.51	0.65	p=0.004
Total outer diameter (distal) (µm)	0.51±0.15	0.67±0.31	0.42±0.13	p=0.044
Inner axonal diameter (distal) (µm)	0.37±0.15	0.39±0.13	0.27±0.11	p=0.116
g-ratio (distal)	0.72‡	0.58	0.64	p=0.047

CC Group: control group (nerve lesion repaired by simple entubulation). CC-GHR Group: nerve lesion repaired by entubulation with Ghrelin instillation. CC-ASC Group: nerve lesion repaired by entubulation with conduits seeded with adipose-derived mesenchymal stem cells (ASCs). K-W: Statistical significance by Kruskal-Wallis test. Ultrastructural measurement of total outer diameter and inner axonal diameter in three segments of the sciatic nerve (micrometers). g-ratio: the ratio of the inner axonal diameter to the total outer diameter. †CC vs. CC-GHR-group (p=0.004, Dunn-Bonferroni test); ‡CC vs. CC-GHR-group (p=0.038, Dunn-Bonferroni test). Values are expressed as mean±standard deviation.

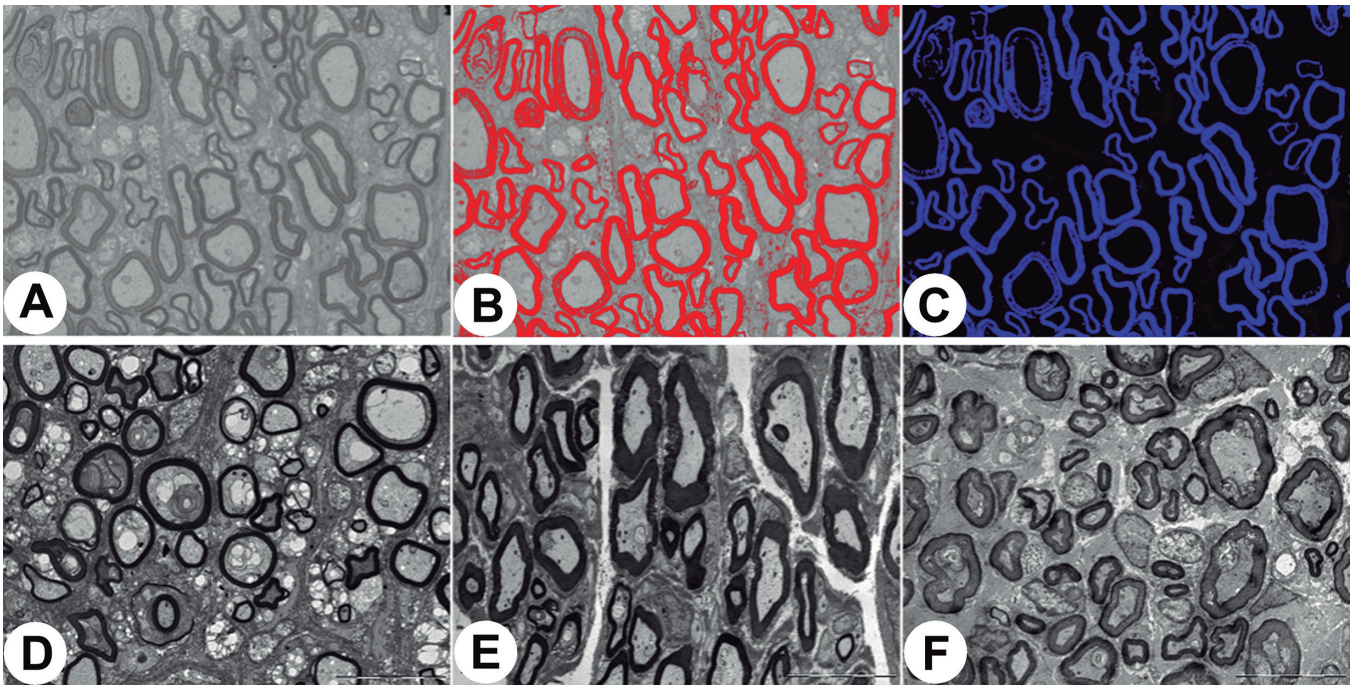

Fig. 4. Ultrastructural analysis of myelin in ultrathin cross-sections of the distal segment of the sciatic nerve. **A-C.** Morphometric procedure used for myelin quantification (normalized and threshold images). **D.** CC group. **E.** CC-GHR group. **F.** CC-ASC group. Note numerous axonal degeneration phenomena in CC group, and higher number of myelinated axons in CC-GHR and CC-ASC groups than in CC-group. Scale bars: 10 μm

fiber area in the distal nerve segment (Spearman's rank correlation coefficient Rho=0.731, p=0.007) and the myelination (g-ratio, Spearman's rank correlation coefficient Rho=0.440, p=0.046).

Discussion

In this experimental study, a model of severe rat sciatic nerve injury was used to explore the effects of GHR and ASCs in combination with a Dl-lactic-ε-caprolactone conduit on the repair of a 10-mm nerve gap. Our data demonstrated that the local administration of GHR around the transected nerve or of ASCs into the nerve conduit induced a greater regeneration of myelinated nerve fibers and a lower reduction in muscle fiber.

The increase in the number of myelinated nerve fibers in the distal segment caused by GHR or ASC treatment did not correlate with a significant improvement in functional recovery, and none of the treated animals reached the preoperative level of ankle kinematics. It should be borne in mind that a higher myelinated fiber count may indicate sprouting rather than an increase in fibers that will eventually innervate muscle. Functional assessment methods have previously yielded variable and controversial results (Varejao et al., 2001, 2004). The presence of edema, ulceration, or mutilations can interfere with the results of systems based on footprint analysis, such as the sciatic function index and static sciatic index (Bain et al., 1989; Bervar, 2000), and the animal rests on the ankle rather than the forefoot in cases of severe functional disorder. ASA analysis, the technique applied in the present study, has demonstrated adequate sensitivity and validity (Dijkstra et al., 2000; Varejao et al., 2001), and its usefulness as an indicator of nerve regeneration is supported by the correlation found between the ASA and the myelinated fiber area in the distal nerve segment (Rho=0.731,

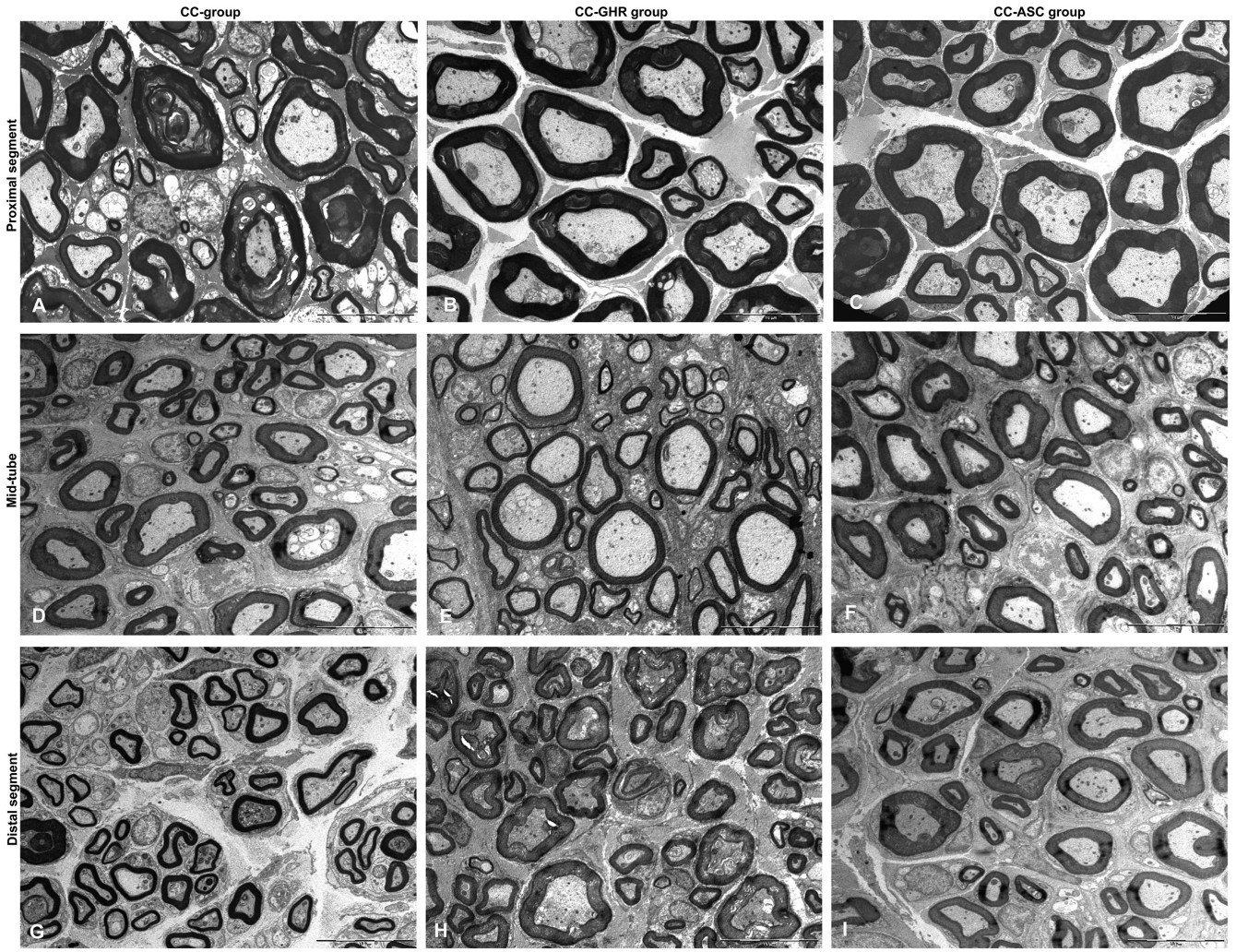

Fig. 5. Representative ultrastructural images of myelin in ultrathin cross-sections of proximal, mid-tube, and distal segments of the sciatic nerve in CC (**A, D, and G**), CC-GHR (**B, E, and H**), and CC-ASC (**C, F, and I**) groups. Scale bars: 10 μm.

p=0.007). A poor functional recovery after peripheral nerve injury has been attributed to the misdirection of regenerating axons and their reinnervation of functionally inappropriate muscles (Hamilton et al., 2011), which may also explain the reduction in muscle wet weight. However, GHR was reported to be effective to prevent posttraumatic skeletal muscle atrophy (Raimondo et al., 2013). Researchers using this experimental model have generally included an electrophysiological study of function (Dornseifer et al., 2011; De Boer et al., 2011). However, given that the histological regeneration of the lesion was the objective of our study, we prioritized the histopathologic and ultrastructural studies and used a simple clinical method to analyze function.

The g-ratio is widely considered to be highly reliable for assessing axonal myelination (Chomiak and Hu, 2009), and the present data are within the range recognized as normal for the sciatic nerve of rat (0.55-0.68) (Chau et al., 2000). We can therefore consider that GHR and ASC treatments have a beneficial effect on remyelination (Table 3).

ASCs were reported to promote peripheral nerve repair (Liu et al., 2011; Carriel et al., 2013) and create a more desirable microenvironment for nerve regeneration (Kingham et al., 2014) in a rat model of nerve resection. Our group studied the effect of another neuropeptide (VIP) in this rat model, finding that its local infusion significantly improved entubulation-induced nerve repair; however, the most favorable axon regeneration outcomes were achieved for the nerve conduit infused with ASCs bearing the VIP transcript (Hernández-Cortés et al., 2014).

Various mechanisms may underlie the effect of GHR on peripheral nerve repair observed in our study. GHR is known to be a potent neurotrophic factor in the central nervous system, especially in degenerative and lesion conditions (Stoyanova et al., 2013; Qi et al., 2014). This mechanism is likely to contribute to the beneficial effect of GHR in nerve repair, although its role at peripheral level has yet to be demonstrated. A pilot study showed a significantly more rapid functional recovery by Myh6/Ghrl transgenic mice after median nerve transection and immediate repair (Raimondo et al., 2013), suggesting that GHR also promotes axonal regeneration after nerve injury and repair. The present morphologic, immunohistochemical, and ultrastructural results also indicate that GHR improves axonal regeneration. However, nerve injury damages both nerve (axons and Schwann cells) and connective (epineural, perineural and endoneural) tissues, which compete to occupy the space between nerve ends; therefore, the proliferation of connective tissue can interfere with axonal regeneration. In this context, the anti-inflammatory activity of GHR (Gonzalez-Rey and Delgado, 2007; Anderson and Delgado, 2008) is expected to reduce the local inflammatory reaction and consequently the post-traumatic perineural fibrosis. Indeed, GHR infusion in the entubulated nerve reduced the area of perineural fibrosis in the distal segment of the sciatic nerve, and this effect would contribute to its neurotrophic action. Other researchers associated the anti-inflammatory action of GHR with a reduction in nerve damage and neuropathic pain sensitization in models of diabetes-induced polyneuropathy and sciatic nerve constriction (Guneli et al., 2010; Tsuchimochi et al., 2013).

Interestingly, the nerves repaired with ASC-seeded conduits showed larger areas of perineural fibrosis. This was unexpected, because ASCs exert anti-fibrotic effects in many systems. Given that ASCs show preferential tropism for sites of inflammation and injury (Gonzalez et al., 2009), it is likely that ASCs remained in the conduit for a long period after their infusion. Further studies are required to confirm whether the perineural connective tissue corresponds to ASCs engrafted in the nerve.

The generally short half-life and consequent low availability of proteins (e.g., GHR) in vivo potentially limit their utilization in nerve conduits. Systems employed to achieve the long-term delivery of nerve growth factor (NGF) have included impregnated fibronectin mats (Whitworth et al., 1996), fibrin matrices (Lee et al., 2003), fibrin sealant (Jubran and Widenfalk, 2003), gelatin-tricalcium phosphate membranes (Chen et al., 2006), growth factor eluting conduits (Yu and Bellamkonda, 2003), subcutaneous reservoir implantation for infusion at the coaptation site (Santos et al., 1998), and mini-osmotic pumps (Young et al., 2001). De Boer et al. (2011) recently addressed the availability problem by using microspheres to deliver NGF in a poly-lactic-co-glycolic-acid nerve conduit. Research efforts have lately focused on generating more stable analogs of GHR for future applications in different clinical settings.

Taken together, the present data indicate that GHR and ASCs have a mild positive effect on repair by entubulation in peripheral nerve injuries.

Conclusion: These results suggest that the utilization of ghrelin or ASCs may improve nerve regeneration with Dl-lactic-ε-caprolactone conduits. Further research is warranted to establish the usefulness of this approach for the clinical repair of peripheral nerve lesions.

Acknowledgements. The authors would especially like to acknowledge the contribution to the histochemical and immunohistochemical studies of Serafín Vélez García and Carmen Ruiz Guzman, technicians in the Surgical Department, and María Dolores Rodríguez, in the Pathology Department and IBIMER of Granada University. This investigation was supported in part by Research Group #CTS-138 (Junta de Andalucía, Spain).

Disclaimers. The authors have no direct or indirect financial interests in the products listed in the study. F. O'Valle is one of the intellectual authors of the Fibrosis HR® program.

References

Anderson P. and Delgado M. (2008). Endogenous anti-inflammatory

neuropeptides and pro-resolving lipid mediators: a new therapeutic approach for immune disorders. J. Cell. Mol. Med. 12, 1830-1847.

Ansselin A.D., Fink T. and Davey D.F. (1998). An alternative to nerve grafts in peripheral nerve repair: Nerve guides seeded with adult Schwann cells. Acta Chir. Austriaca 30, 19-24.

Ao Q., Fung C.K., Tsui A.Y., Cai S., Zuo H.C., Chan Y.S. and Shum D.K. (2011). The regeneration of transected sciatic nerves of adult rats using chitosan nerve conduits seeded with bone marrow stromal cell-derived Schwann cells. Biomaterials 32, 787-796.

Araña M., Mazo M., Aranda P., Pelacho B. and Prosper F (2013). Adipose tissue-derived mesenchymal stem cells: Isolation, expansion, and characterization. Methods Mol Biol. 1036, 47-61

Babu P., Behl A., Chakravarty B., Bhandari P.S., Bhatti T.S. and Maurya S. (2008). Entubulation techniques in peripheral nerve repair. Indian J. Neurotrauma. 5, 15-20.

Bain J.R., Mackinnon S.E. and Hunter D.A. (1989). Functional evaluation of complete sciatic, peroneal, and posterior tibial nerve lesions in the rat. Plast. Reconstr. Surg. 83, 129-138.

Belkas J., Munro C.A., Shoichet M.S. and Midha R. (2005). Peripheral nerve regeneration through a synthetic hydrogel nerve tube. Restor. Neurol. Neurosci. 23, 19-29.

Bervar M. (2000). Video analysis of standing--an alternative footprint analysis to assess functional loss following injury to the rat sciatic nerve. J. Neurosci. Methods 102, 109-116.

Carriel V., Garrido-Gómez J., Hernández-Cortés P., Garzón I., García-García S., Sáez-Moreno J.A., Sánchez-Quevedo M.C., Campos A. and Alaminos M. (2013). Combination of fibrin-agarose hydrogels and adipose-derived mesenchymal stem cells for peripheral nerve regeneration. J. Neural Eng. 10, 026022.

Chau W.K., So K.F., Tay D. and Dockery P. (2000). A morphometric study of opticaxons regenerated in a sciatic nerve graft of adult rats. Restor Neurol. Neurosci. 16, 105-116.

Chen M.H., Chen P.R., Chen M.H., Hsieh S.T. and Lin F.H. (2006). Gelatin-tricalcium phosphate membranes immobilized with NGF, BDNF, or IGF-1 for peripheral nerve repair: An in vitro and in vivo study. J. Biomed. Mater. Res. A 79, 846-857.

Chomiak T. and Hu B. (2009). What Is the optimal value of the g-ratio for myelinated fibers in the rat CNS? A Theoretical Approach. PLoS ONE 4, e7754.

De Boer R., Knight A.M., Borntraeger A., Hébert-Blouin M.N., Spinner R.J., Malessy M.J.A., Yaszemski M.J. and Windebank A.J. (2011). Rat sciatic nerve repair with a poly-lactic-co-glycolic acid scaffold and nerve growth factor releasing microspheres. Microsurgery 31, 293-302.

Delporte C. (2013). Structure and physiological actions of ghrelin. Scientifica (Cairo). 2013, 518909.

di Summa P.G., Kingham P.J., Raffoul W., Wiberg M., Terenghi G. and Kalbermatten D.F. (2010). Adipose-derived stem cells enhance peripheral nerve regeneration. J. Plast. Reconstr Aesthet Surg. 63, 1544-1552.

Dijkstra J.R., Meek M.F., Robinson P.H. and Gramsbergen A. (2000). Methods to evaluate functional nerve recovery in adult rats: walking track analysis, video analysis and the withdrawal reflex. J. Neurosci. Methods 96, 89-96.

Dornseifer U., Fichter A.M., Leichtle S., Wilson A., Rupp A., Rodenacker K., Minkovic M., Biemer E., Machens H.G., Matiasek K. and Papadopulos N.A. (2011). Peripheral nerve reconstruction with collagen tubes filled with denatured autologous muscle tissue in the rat model. Microsurgery 31, 632-641.

Gonzalez M.A., Gonzalez-Rey E., Rico L., Büscher D. and Delgado M. (2009). Adipose-derived mesenchymal stem cells alleviate experimental colitis by inhibiting inflammatory and autoimmune responses. Gastroenterology 136, 978-989.

Gonzalez-Rey E. and Delgado M. (2007). Anti-inflammatory neuropeptide receptors: new therapeutic targets for immune disorders? Trends Pharmacol. Sci. 28, 482-491.

Gonzalez-Rey E., Anderson P., González M.A., Rico L., Büscher D. and Delgado M. (2009). Human adult stem cells derived from adipose tissue protect against experimental colitis and sepsis. Gut 58, 929-939.

Guneli E., Onal A., Ates M., Bagriyanik H.A., Resmi H., Orhan C.E., Kolatan H.E. and Gumustekin M. (2010). Effects of repeated administered ghrelin on chronic constriction injury of the sciatic nerve in rats. Neurosci. Lett. 479, 226-230.

Hamilton S.K., Hinkle M.L., Nicolini J., Rambo L.N., Rexwinkle A.M., Rose S.J., Sabatier M.J., Backus D. and English A.W. (2011). Misdirection of regenerating axons and functional recovery following sciatic nerve injury in rats. J. Comp. Neurol. 519, 21-33.

Hobson C.M.I., Green C.J. and Terenghi G. (2000). VEGF enhances intraneural angiogenesis and improves nerve regeneration after axotomy. J. Anat. 197, 591-605.

Hernández-Cortés P., Toledo-Romero M.A., Delgado M., Sánchez-González C.E., Martin F., Galindo Moreno P. and O'Valle F. (2014). Peripheral nerve reconstruction with epsilon-caprolactone conduits seeded with vasoactive intestinal peptide gene-transfected mesenchymal stem cells in a rat model. J. Neural. Eng. 11, 046024.

Jubran M. and Widenfalk J. (2003). Repair of peripheral nerve transections with fibrin sealant containing neurotrophic factors. Exp. Neurol. 181, 204-212.

Kim S.M., Lee S.K. and Lee J.H. (2007). Peripheral nerve regeneration using a three dimensionally cultured Schwann cell conduit. J. Craniofac. Surg. 18, 475-488.

Kingham P.J., Kolar M.K., Novikova L.N., Novikov L.N. and Wiberg M. (2014). Stimulating the neurotrophic and angiogenic properties of human adipose-derived stem cells enhances nerve repair. Stem Cells Dev. 23, 741-754.

Lee A.C., Yu V.M., Lowe J.B. 3rd, Brenner M.J., Hunter D.A., Mackinnon S.E. and Sakiyama-Elbert S.E. (2003). Controlled release of nerve growth factor enhances sciatic nerve regeneration. Exp. Neurol. 184, 295-303.

Liu G.B., Cheng Y.X., Feng Y.K., Pang C.J., Li Q., Wang Y., Jia H. and Tong X.J. (2011). Adipose-derived stem cells promote peripheral nerve repair. Arch. Med. Sci. 7, 592-596.

Masseroli M., O'Valle F., Andújar M., Ramírez C., Gómez-Morales M., de Dios Luna J., Aguilar M., Aguilar D., Rodríguez-Puyol M. and Del Moral R.G. (1998). Design and validation of a new image analysis method for automatic quantification of interstitial fibrosis and glomerular morphometry. Lab. Invest. 78, 511-522.

Meek M.F., van der Werff J.F., Klok F., Robinson P.H., Nicolai J.P. and Gramsbergen A. (2003). Functional nerve recovery after bridging a 15 mm gap in rat sciatic nerve with a biodegradable nerve guide. Scand. J. Plast. Reconstr. Surg. Hand Surg. 37, 258-265.

Qi L., Cui X., Dong W., Barrera R., Coppa G.F., Wang P. and Wu R. (2014). Ghrelin protects rats against traumatic brain injury and hemorrhagic shock through upregulation of UCP2. Ann. Surg. 260, 169-178.

Raimondo S., Ronchi G., Geuna S., Pascal D., Reano S., Filigheddu N. and Graziani A. (2013). Ghrelin: a novel neuromuscular recovery

promoting factor? Int. Rev. Neurobiol. 108, 207-221.

Santos X., Rodrigo J., Hontanilla B. and Bilbao G. (1998). Evaluation of peripheral nerve regeneration by nerve growth factor locally administered with a novel system. J. Neurosci. Methods 85, 119-127.

Stoyanova I.I., le Feber J. and Rutten W.L. (2013). Ghrelin stimulates synaptic formation in cultured cortical networks in a dose-dependent manner. Regul. Pept. 186, 43-48.

Strauch B. (2000). Use of nerve conduits in peripheral nerve repair. Hand Clin. 16, 123-130.

Timmer M., Robben S., Müller-Ostermeyer F., Nikkhah G. and Grothe C. (2003). Axonal regeneration across long gaps in silicone chambers filled with Schwann cells overexpressing high molecular weight FGF-2. Cell Transplant. 12, 265-277.

Tsuchimochi W., Kyoraku I., Yamaguchi H., Toshinai K., Shiomi K., Kangawa K. and Nakazato M. (2013). Ghrelin prevents the development of experimental diabetic neuropathy in rodents. Eur. J. Pharmacol. 702, 187-193.

Varejao A.S., Cabrita A.M., Patricio J.A., Bulas-Cruz J., Gabriel R.C., Melo-Pinto P., Couto P.A. and Meek M.F. (2001). Functional assessment of peripheral nerve recovery in the rat: gait kinematics. Microsurgery 21, 383-388.

Varejao A.S., Melo-Pinto P., Meek M.F., Filipe V.M. and Bulas-Cruz J. (2004). Methods for the experimental functional assessment of rat sciatic nerve regeneration. Neurol. Res. 26, 186-194.

Whitworth I.H., Brown R.A., Dore C.J., Anand P., Green C.J. and Terenghi G. (1996). Nerve growth factor enhances nerve regeneration through fibronectin grafts. J. Hand Surg. Br. 21, 514-522.

Young C., Miller E., Nicklous D.M. and Hoffman J.R. (2001). Nerve growth factor and neurotrophin-3 affect functional recovery following peripheral nerve injury differently. Restor. Neurol. Neurosci. 18, 167-175.

Yu H., Peng J., Guo Q., Zhang L., Li Z., Zhao B., Sui X., Wang Y., Xu W. and Lu S. (2009). Improvement of peripheral nerve regeneration in acellular nerve grafts with local release of nerve growth factor. Microsurgery 29, 330-336.

Yu X. and Bellamkonda R.V. (2003). Tissue-engineered scaffolds are effective alternatives to autografts for bridging peripheral nerve gaps. Tissue Eng. 9, 421-430.

Accepted September 30, 2016